

† SUPPORTING INFORMATION

Structure and electrochemical properties of novel mixed Li(Fe_{1-x}M_x)SO₄F (M = Co, Ni, Mn) phases fabricated by low temperature ionothermal synthesis†

**Prabeer Barpanda,^a Nadir Recham,^a Jean-Nöel Chotard,^a
Karim Djellab,^a Wess Walker,^b
Michel Armand^a and Jean-Marie Tarascon^{*a,c}**

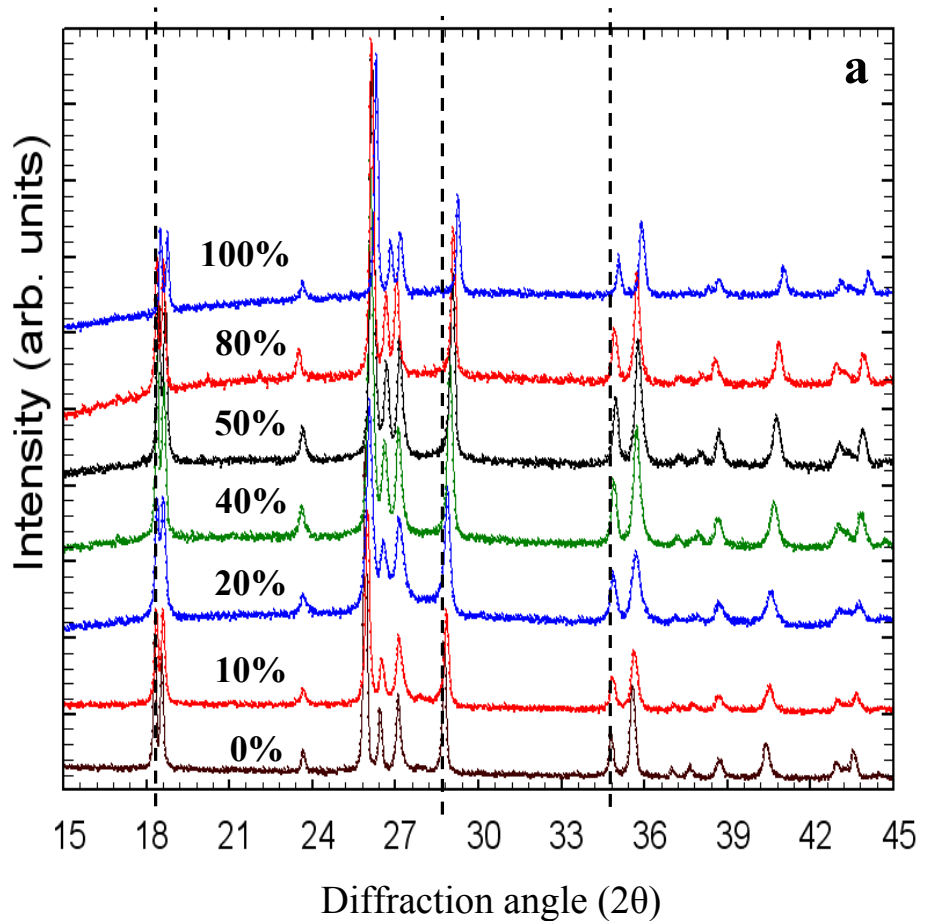
^a Laboratoire de Réactivité et Chimie des Solides, UMR 6007,
Université de Picardie Jules Verne, 80039 Amiens, France

^b Visiting Post-Doctorate, ^c Visiting Professor, Materials Department,
University of California Santa Barbara, CA 93106, USA

** author for correspondence: jean-marie.tarascon@sc.u-picardie.fr*

List of Supporting Information

- Fig. S1** XRD patterns of (a) (Fe_{1-x}Co_x)SO₄.H₂O and (b) (Fe_{1-x}Mn_x)SO₄.H₂O monohydrate precursors with different compositions.
- Table S1** Lattice parameters and cell volume of (Fe_{1-x}Co_x)SO₄.H₂O solid-solution precursors having monoclinic (*C2/c*) symmetry.
- Table S2** Lattice parameters and cell volume of (Fe_{1-x}Mn_x)SO₄.H₂O solid-solution precursors having monoclinic (*C2/c*) symmetry.
- Fig. S2** Some additional SEM images of Li(Fe_{1-x}M_x)SO₄F compounds.
- Fig. S3** Some representative EDAX elemental analysis of Li(Fe_{1-x}Mn_x)SO₄F compounds.
- Fig. S4** Galvanostatic electrochemical cycling profiles of (a) Li(Fe_{0.9}Mn_{0.1})SO₄F, (b) Li(Fe_{0.8}Mn_{0.2})SO₄F compounds.



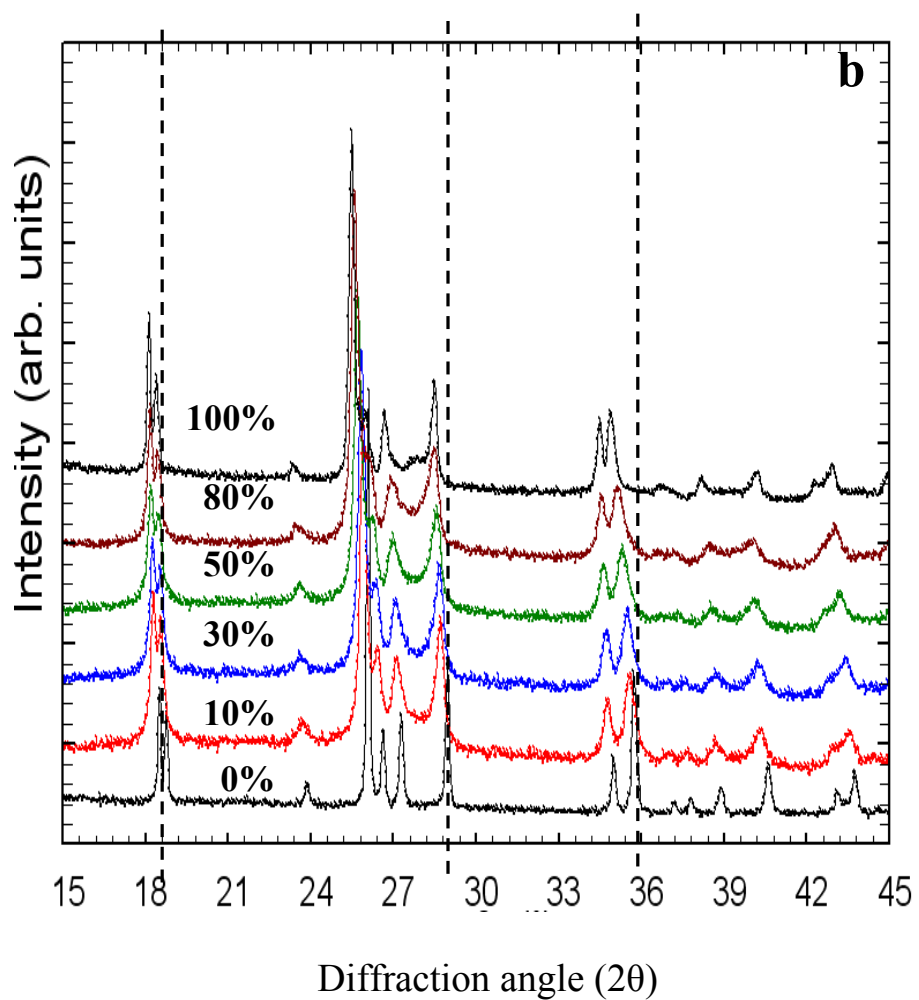


Fig. S1 X-ray diffraction patterns of (a) $(Fe_{1-x}Co_x)SO_4 \cdot H_2O$ and (b) $(Fe_{1-x}Mn_x)SO_4 \cdot H_2O$ monohydrate precursors varying the Co or Mn doping content from 0 to 100 wt%. The numbers alongside the diffraction patterns present the Co or Mn dopant content (wt%). As shown, increasing Co content gradually leads to lower lattice volume as indicated by peak shift towards higher diffraction angle (or lower d value) due to the lower ionic radii of Co wrt Fe (similar to Ni doping in the manuscript Fig 2). On the other hand, Mn doping shifts the XRD peaks towards lower angle (or higher d value) reflecting the larger ionic radii of Mn wrt Fe. The dashed lines are shown to guide eyes about the gradual peak shift upon varying the precursor composition.

Table S1 Lattice parameters and cell volume of $(Fe_{1-x}Co_x)SO_4 \cdot H_2O$ solid-solution precursors having monoclinic ($C2/c$) symmetry.

Materials	a (Å)	b (Å)	c (Å)	V (Å ³)	β (°)
FeSO ₄ .H ₂ O	7.0918(3)	7.5352(2)	7.7822(2)	364.67(2)	118.72(2)
(Fe _{0.90} Co _{0.10})SO ₄ .H ₂ O	7.0845(2)	7.5429(1)	7.7645(1)	364.09(1)	118.66(1)
(Fe _{0.60} Co _{0.40})SO ₄ .H ₂ O	7.0904(2)	7.5864(2)	7.7145(1)	362.36(1)	119.16(5)
(Fe _{0.50} Co _{0.50})SO ₄ .H ₂ O	7.0405(2)	7.5553(2)	7.6875(1)	357.80(1)	118.95(1)
(Fe _{0.40} Co _{0.60})SO ₄ .H ₂ O	7.0246(1)	7.5620(1)	7.6753(1)	356.77(1)	118.86(2)
(Fe _{0.20} Co _{0.80})SO ₄ .H ₂ O	6.9866(6)	7.5498(6)	7.6353(4)	352.93(4)	118.80(1)
CoSO ₄ .H ₂ O	6.9542(8)	7.5731(1)	7.6242(1)	351.72(3)	118.68(1)

Table S2 Lattice parameters and cell volume of $(Fe_{1-x}Mn_x)SO_4 \cdot H_2O$ solid-solution precursors having monoclinic ($C2/c$) symmetry.

Materials	a (Å)	b (Å)	c (Å)	V (Å ³)	β (°)
FeSO ₄ .H ₂ O	7.0918(3)	7.5352(2)	7.7822(2)	364.67(2)	118.72(2)
(Fe _{0.90} Mn _{0.10})SO ₄ .H ₂ O	7.1279(2)	7.5305(2)	7.7921(1)	366.37(2)	118.84(5)
(Fe _{0.70} Mn _{0.30})SO ₄ .H ₂ O	7.1342(2)	7.4689(2)	7.8862(1)	367.19(1)	119.09(5)
(Fe _{0.50} Mn _{0.50})SO ₄ .H ₂ O	7.1592(3)	7.5473(3)	7.8404(2)	370.35(2)	119.05(2)
(Fe _{0.20} Mn _{0.80})SO ₄ .H ₂ O	7.1425(2)	7.4985(2)	7.7248(2)	372.48(2)	115.80(3)
MnSO ₄ .H ₂ O	7.1241(6)	7.6631(4)	7.7642(7)	381.44(3)	115.85(12)

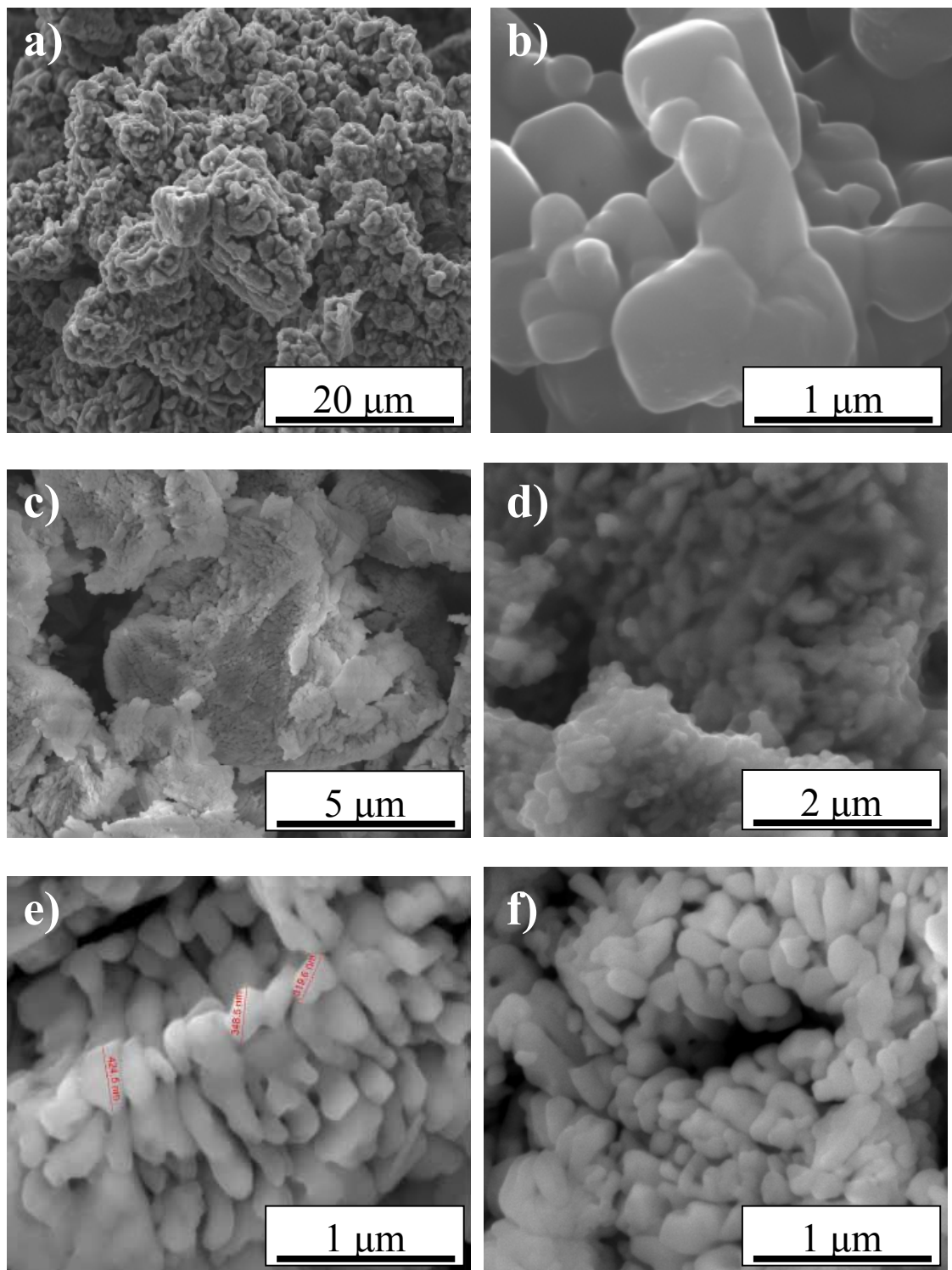


Fig. S2 SEM images showing the topotactic reaction involving initial $(\text{Fe}_{1-x}\text{M}_x)\text{SO}_4\cdot\text{H}_2\text{O}$ precursor and final $\text{Li}(\text{Fe}_{1-x}\text{M}_x)\text{SO}_4\text{F}$ products with similar morphology. (a) $(\text{Fe}_{0.80}\text{Co}_{0.20})\text{SO}_4\cdot\text{H}_2\text{O}$, (b) $\text{Li}(\text{Fe}_{0.80}\text{Co}_{0.20})\text{SO}_4\text{F}$, (c) $(\text{Fe}_{0.80}\text{Ni}_{0.20})\text{SO}_4\cdot\text{H}_2\text{O}$, (d) $\text{Li}(\text{Fe}_{0.80}\text{Ni}_{0.20})\text{SO}_4\text{F}$, e) $(\text{Fe}_{0.90}\text{Ni}_{0.10})\text{SO}_4\cdot\text{H}_2\text{O}$ and f) $\text{Li}(\text{Fe}_{0.90}\text{Ni}_{0.10})\text{SO}_4\text{F}$.

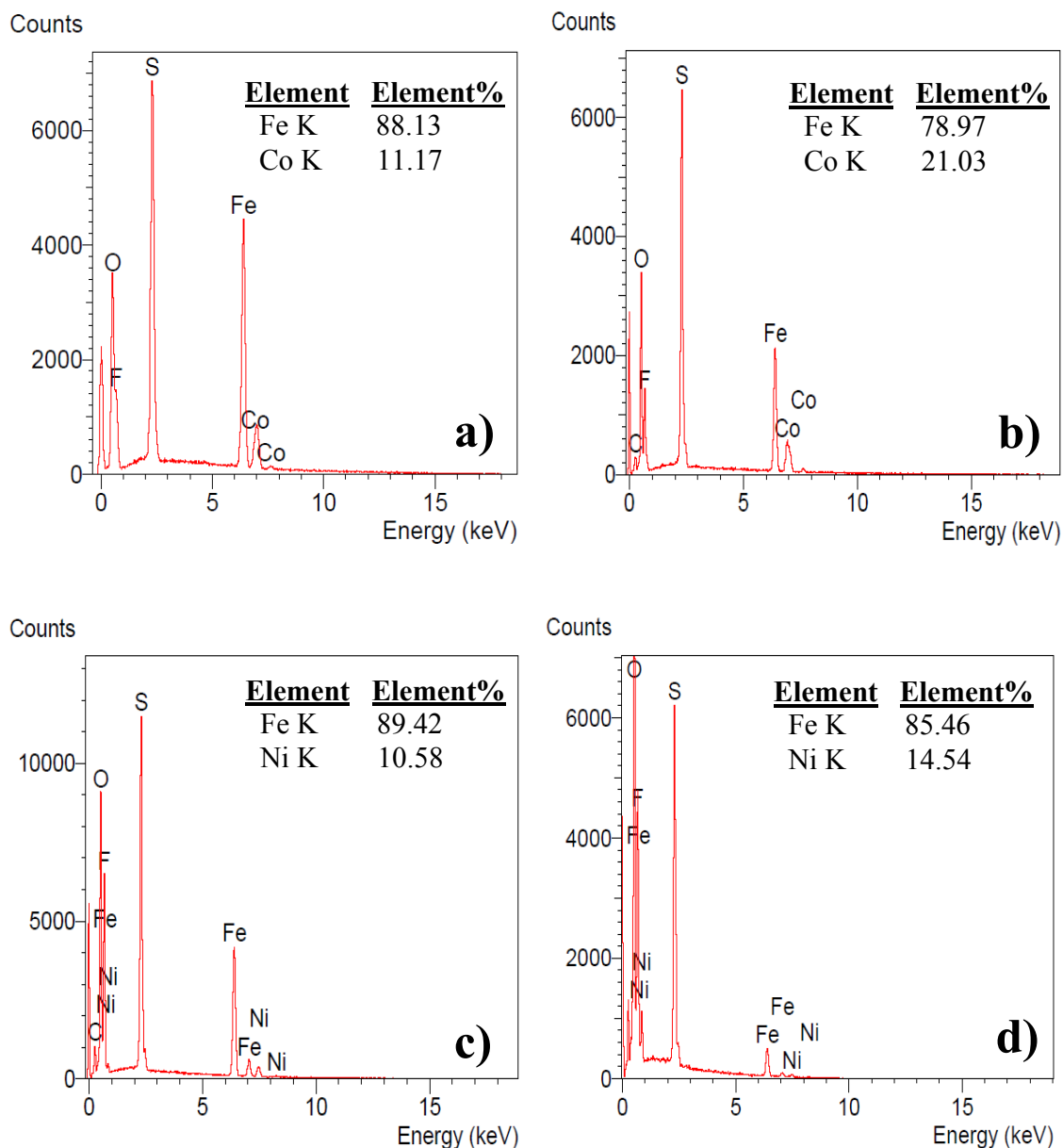


Fig. S3 Some representative EDAX elemental analysis done in conjunction with SEM study to confirm the stoichiometric composition and uniform distribution of individual $3d$ transition metals in $\text{Li}(\text{Fe}_{1-x}\text{M}_x)\text{SO}_4\text{F}$ products; (a) $\text{Li}(\text{Fe}_{0.90}\text{Co}_{0.10})\text{SO}_4\text{F}$, (b)

$\text{Li}(\text{Fe}_{0.80}\text{Co}_{0.20})\text{SO}_4\text{F}$, (c) $\text{Li}(\text{Fe}_{0.90}\text{Ni}_{0.10})\text{SO}_4\text{F}$ and (d) $\text{Li}(\text{Fe}_{0.80}\text{Ni}_{0.20})\text{SO}_4\text{F}$ products. The elemental analysis values are enlisted in the inset of each figure.

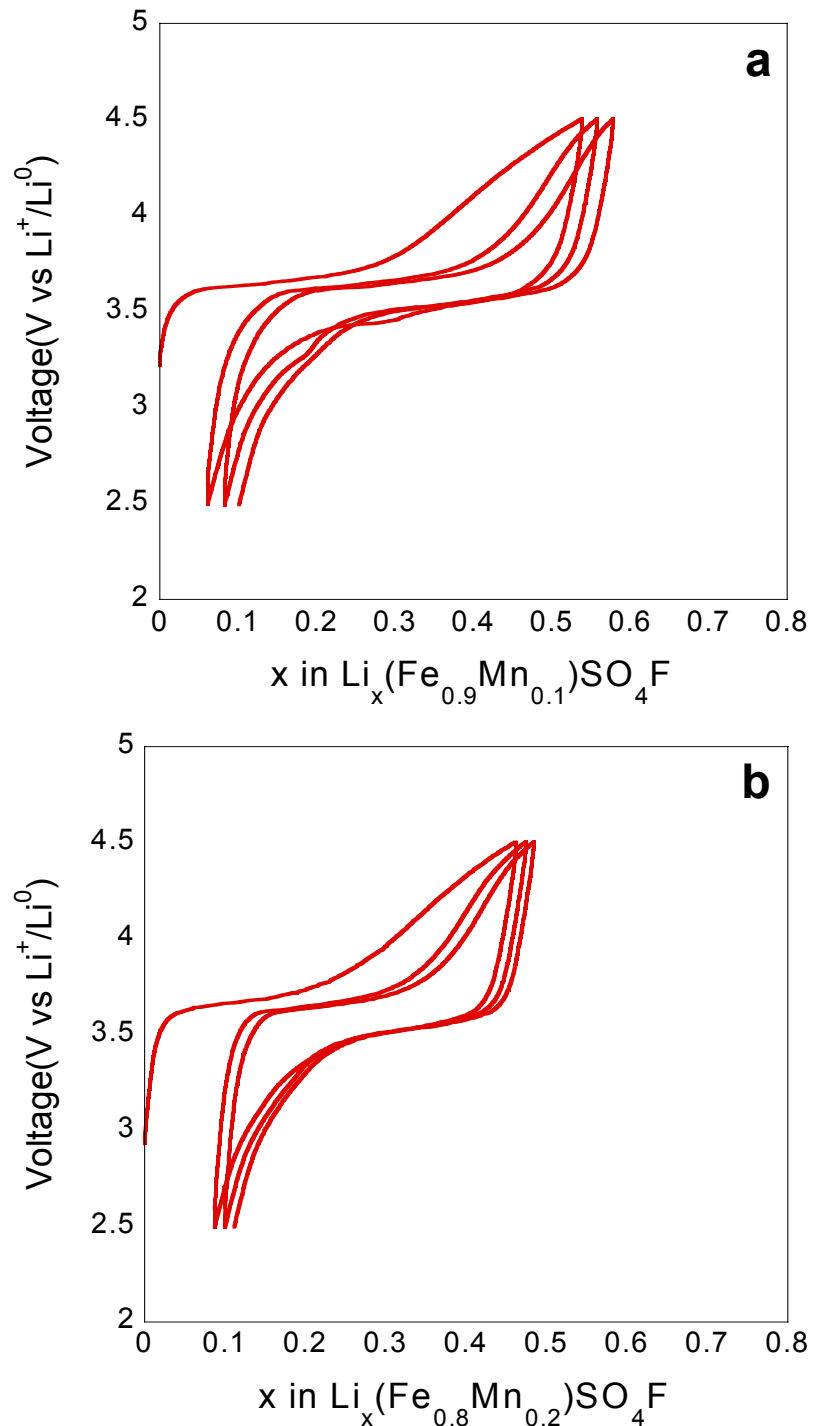


Fig. S4 Galvanostatic electrochemical cycling profiles of (a) $\text{Li}(\text{Fe}_{0.9}\text{Mn}_{0.1})\text{SO}_4\text{F}$, (b) $\text{Li}(\text{Fe}_{0.8}\text{Mn}_{0.2})\text{SO}_4\text{F}$ compounds, cycled between 2.5 to 4.5 V at C/10 (1 Li in 10 hours) in Li-half cell swagelok setting. The electrodes were prepared by ball-milling

Supplementary material (ESI) for Journal of Materials Chemistry
This journal is © The Royal Society of Chemistry 2010

Li(Fe_{1-x}Mn_x)SO₄F and carbon black (85:15 weight ratio) for 15 minutes. A 3.6 V plateau is observed in both cases with excellent cycling stability.